Advances in Engineering Research, volume 208
Proceedings of the International Conference on Innovation in Science and Technology (ICIST 2020)

Preliminary Modelling of a CubeSat Attitude Control System Using a Reaction Wheel

Linda Nur Afifa[1,2]
[1]Department of Information Technology
Darma Persada University
Jakarta, Indonesia
[2]Department of Computer Science and Electronics
Gadjah Mada University
Yogyakarta, Indonesia
afycena@gmail.com

Tri Kuntoro Priyambodo*, Andi Dharmawan
Department of Computer Science and Electronics
Gadjah Mada University
Yogyakarta, Indonesia
*mastri@ugm.ac.id, andi_dharmawan@ugm.ac.id

***Abstract*—Stabilization of satellite attitude is the most important thing that should always be maintained during orbit. A model of satellite stillness controllers fairly stable against interference and simple has been developed. This is evidenced by testing models to control motion on the Z-axis. A Proportional Integral (PI) controller has been selected as the actuator controller. By tuning parameters P=423.6 and I=693.7, producing relatively good system characteristics, the maximum overshoot (M_P) decreases by 3%, and the rise time improves (t_r=3.1s), but the settling time increases. By making a few modifications, this model can be used as a basis for transferring motion control to other axes—i.e., the X-axis (roll) and Y-axis (pitch).**

Keywords—CubeSat, ACS modeling, reaction wheel, PI controller

I. INTRODUCTION

A CubeSat is a satellite with a standard size of 10 x 10 x 10 cm^3 and a maximum weight of 1.33 kg, categorized into nanosatellite [1-3]. After launch, such a satellite must remain in a designated orbit and orientation. For this, an Attitude Control System (ACS) is necessary.

ACS has two functions, first, to produce external torque to direct satellites, and second, to exchange momentum. The most widely used momentum exchange device is the reaction wheel. Although this device has a fairly high accuracy level, it cannot be very easy because it requires considerable power.

A reaction wheel is an actuator that works based on the principle of angular momentum. It employs a DC motor mounted on a central flywheel, located at all three satellite axes [4]. This rotating motor produces the torque required by the satellite, and a change in angular velocity affects the motion and orientation of the satellite.

However, reaction wheels have a notable weakness, i.e., saturation [5], which occurs when a change in momentum exceeds the storage capacity of the satellite [6,7]. Saturation is closely related to the motor's maximum speed and is usually limited by the reaction wheel's maximum voltage [8].

Due to these limitations, reaction wheels cannot perform optimally, decreasing work performance [9]. Internal and external interference, such as gravity torque, radiation torque, and environmental torque, may further limit the control system's accuracy [10].

Following CubeSat's mission, modelling is required to develop an appropriate ACS model and ensure its availability. This article provides such modeling. According to the specified reference, ACS controls satellite motion on three axes, i.e., X, Y, and Z axes. The control process is carried out sequentially, depending on the sequence of satellite rotation. In this study, the satellite rotation was modeled in the sequence of 323 or ZYZ, i.e., rotated on the Z-axis, then the Y-axis, then to the Z-axis. It is therefore modeled rotation control on the Z-axis.

The satellite attitude control modeling described in this paper begins by explaining how inertia and body frame are used. Then proceed with the equation's derivation for the satellite body's motion, actuators, and controllers. Furthermore, the model equation is simulated using software to see its characteristics. By looking at the model's system characteristics, it can be concluded that the model is good or not, can be implemented or not.

This paper is organized into five sections. Section 1, the introduction, explains the research background, Section describes related work, including previous research related to ACS modeling. Section 3, ACS modeling, contains a derivation of mathematical equations for actuators, satellite bodies, and control systems. Section 4 presents the simulation and discussion, while Section 5 offers several conclusions.

II. RELATED WORK

The reaction wheel is one of the main components of ACS, which is the source of disturbance [11], usually caused by

flywheel imbalance, ripple torque, and friction to interfere with the accuracy and stability satellite [12].

Reaction wheels are the most widely used actuators; it has highly accurate and produces precise torque, making them suitable for satellites that require high-speed maneuvering [13-15]. Stabilization is an important issue that should be considered at the time of ACS design [16].

In existing research [17,18], ACS has been modeled by modeling the satellite body and the actuators used, i.e., reaction wheels, and using the results to analyze system stability. The control system often used to handle stabilization issues is PID [19-21].

PID control systems are widely used to control the motion of a system, such as vertical motion UAV [22], for VTOL stabilization [23], to maintain quadrotor flight [24], namely by tuning coefficients P, I, and D and can be optimized in value by other methods such as Ant Colony, PSO, and others.

III. ACS MODELING

In this section, the physical motion modeling of the satellite body, actuator, and controller will be described within the context of ACS modeling. For modeling, several system dynamics are required: the inertia framework, the motion frame, and the body frame. The inertia framework is labeled $X_G - Y_G - Z_G$. The point of origin is the center of the earth, the X_G axis faces the vernal equinox, the Y_G axis indicates north, direction, and Z_G rotates using the right-hand rule, as described in figure 1.

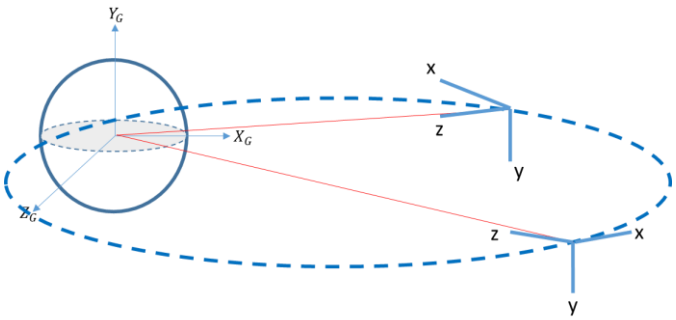

Fig. 1. Inertia framework.

The body frame describes the position of the object's body when rotating in three axes, namely the x-axis (roll), the Y-axis (pitch), and the Z-axis (yaw), as described in Figure 2. The torque is generated on each axis, expressed by equation 1-3. ACS controls satellite torque on roll, pitch and yaw axes. In this simulation, the torque to be controlled is the torque on the Z-axis.

$$T_{dx} + T_{cx} = I\ddot{\varphi} \quad (1)$$

$$T_{dy} + T_{cy} = I\ddot{\theta} \quad (2)$$

$$T_{dz} + T_{cz} = I\ddot{\psi} \quad (3)$$

Inertia frameworks, dynamics equations, and body frames are used as the basis for modeling the plant. The plant consists of the actuators and processes to be controlled. System performance is measured using the transfer function.

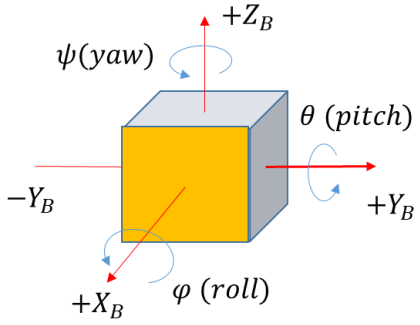

Fig. 2. Body framework.

A. Satellite Body Motion Modeling

Satellite dynamics are defined by Equation 4.

$$J\ddot{\theta} + B\dot{\theta} = T_m \quad (4)$$

Where $\boldsymbol{J}$ is satellite inertia, $\boldsymbol{B}$ is satellite dumping, and $\boldsymbol{T_m}$ is motor torque. By changing Equation 1 using the Laplace transform, output and input torque were compared, as expressed in Equation 5 and Equation 6.

$$JS^2\theta(s) + BS\theta(s) = T_m \quad (5)$$

$$\frac{\theta(s)}{T_m} = \frac{1}{JS^2+BS} \quad (6)$$

B. Actuator Modeling

The actuator used to drive the satellite is the reaction wheel, a DC motor [14,17,18]. DC motors are actuators that produce angular acceleration on flywheels, thereby producing torque and angular momentum that can change the satellite's orientation. Change in momentum is generated by the reaction wheel to move the satellite in the opposite direction.

DC motor modeling is grouped into three elements: the electrical system, the mechanical system, and the rotational system, as expressed in Equation 7.

$$T_m(S) = T_L(S) + T_d(S) \quad (7)$$

$\boldsymbol{T_L}$ is load torque, $\boldsymbol{T_d}$ is the internal disturbance torque motor; in this initial study, the disturbance was ignored. By using the Laplace transform, Equation 8 was obtained.

$$\frac{\theta(S)}{V_O(S)} = \frac{K}{(Js+b)(R_a+L_aS)} \quad (8)$$

C. *Disturbance*

Frequently interfering with low-orbit satellites (LEO) are gravity gradient (T_g), magnetic torque (T_m), aerodynamic torque (T_a), and solar radiation (T_s) [1,25,26].

In this study, total disturbance torque was used as a reference; satellites should produce torque that is at least twice as much as disturbance torque. In this study, the total amount used was 6.850 10-7[Nm], the gravity gradient, magnetic torque, aerodynamic torque, and solar radiation.

IV. Simulation and Discussion

Based on the motion modeling of satellite bodies, actuators, controllers, and interference, ACS systems were diagrammed in a transfer function. To identify the ACS characteristics, the parameter values used for each variable of the simulation are given in Table 1.

TABLE I. Variable of Simulation

Variable Simulasi		Magnitude
K_a	Amplifier Gain	10
R_a	Resistance	10 Ohm
L_a	Inductance	0.5 H
J_a	Inertia Motor	0.01 Kg.sqm
J	Inertia Satelit	2.5 Kg.sqm
B	Damping	1.17 Nms
K	DC motor constant	0.01 Nm/s

The results of this modeling of satellite motion, actuators, and control systems were analyzed by looking at the controller's characteristics and the overall output of the model simulation. Figure 3 illustrates the satellite models' output (blue lines) and actuators (red lines) by providing step input. In the image, the settling time is reached at t_s= 3.31, and the output is close to the given input.

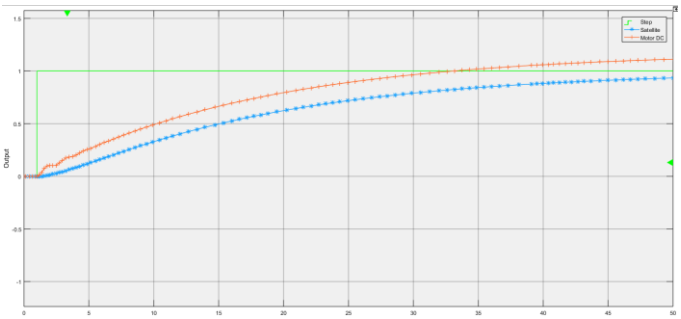

Fig. 3. System output.

Based on the simulation results, this system is stable, as indicated by the equation characteristics of the system being negative (namely -0.5877 + 4.4278i, -0.5877 -4.4278i, -0.3399 + 0.0000i, -0.1527 + 0.0000i).

The analysis is subsequently used to examine the control system's characteristics, using P and I control parameters of 1522 and 1880. The characteristics of the system are graphed in Figure 4. From the figure, it can be seen that rise time starts to increase at $t_r = 1.56\,s$ and that maximum overshoot (M_p=16.3%) exceeds the input value of 1. The system achieves a steady-state (settling time) at $t_s = 7.81s$. The characteristic values of this system are fully presented in Table 2.

The next experiment is used to tune the PI control parameters. The P and I values used in this second experiment were 423.6 and 693.7. Following these parameters, the system characteristics in Figure 5 are generated.

Figure 5 shows a rise time of $t_r = 3.1\,s$, a maximum overshoot of $M_p = 10.5\%$, and a settling time of $t_s = 10.5s$. The complete characteristic values of this simulation can be seen in Table 3.

Figure 4 and Figure 5 show the behavior of the system, as resulting from physical modeling. The output chart first rises to t_r=1.56; after tuning, the control system parameters increases to t_r =3.1. The t_r value is affected by satellite dumping.

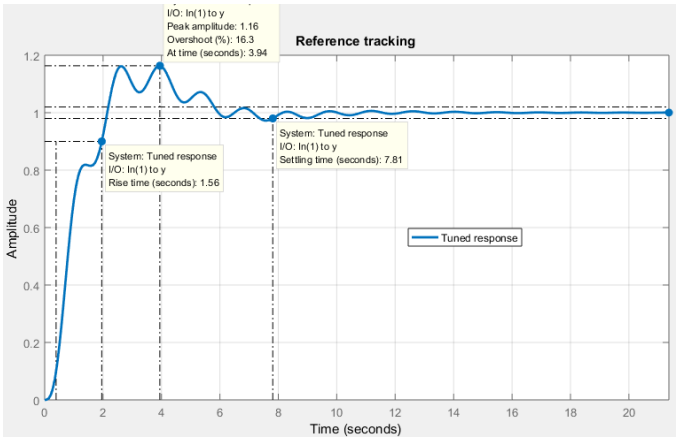

Fig. 4. System characteristics, P=1522, I=1880.

TABLE II. System Characteristics Value

Performance and Robustness		
	Tuned	***Block***
Rise time	1.56 seconds	16.4 seconds
Settling time	7.81 seconds	29 seconds
Overshoot	16.3%	0 %
Peak	1.16%	1
Gain margin	5.45 dB @4.37 rad/s	32.2 dB @4.28 rad/s
Phase margin	60 deg @0.936 rad/s	79.7 deg @ 0.108 rad/s
Closed-loop stability	Stable	Stable

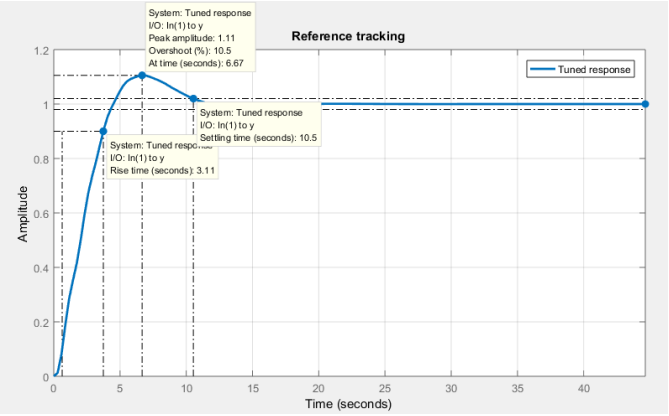

Fig. 5. System characteristics P=423.6, I=693.7.

TABLE III. SYSTEM CHARACTERISTICS VALUE

Performance and Robustness		
	Tuned	***Block***
Rise time	3.1 seconds	16.4 seconds
Settling time	10.5 seconds	29 seconds
Overshoot	10.5 %	0 %
Peak	1.11%	1
Gain margin	16.2 dB @4.32 rad/s	32.2 dB @4.28 rad/s
Phase margin	60 deg @0.448 rad/s	79.7 deg @ 0.108 rad/s
Closed-loop stability	Stable	Stable

Furthermore, the maximum overshoot (**MP**) also decreased by 3%. M_p is an important and necessary value when looking to model a physical system. A good system will not produce much more output than a given input. In the control system, this is represented by the maximum overshoot M_p. In this simulation, the M_p value was 10.5%.

Another important parameter to consider is settling time (t_s), which indicates how quickly a system achieves its final value (usually 2% or 5% of the set value). In the second simulation, t_s increased about 3s. This is an important record at the time of modeling.

V. CONCLUSION

The success of modeling can be ascertained by looking at the system characteristics, i.e., rise time (t_r), settling time (t_s), and maximum overshoot (M_p). Based on the simulation results, the modeling achieved a better maximum overshoot (M_p) after tuning the controller parameters but required more settling time (t_s). It is necessary to review the physical modeling undertaken and the size of the variables given to the system.

ACKNOWLEDGMENT

This research is supported by doctoral dissertation research form The Directorate General of Higher Education, The Indonesian Ministry of Education and Culture through contract number 2086/UN1/DITLIT/DIT-LIT/PT/2020.

REFERENCES

[1] E. Oland and R. Schlanbusch, “Reaction Wheel Design for CubeSat,” in 4th International Conference on Recent Advances in Space Technologies, Istanbul, 2009, pp. 778–783, 2009.

[2] The Tauri Group, “State of the Satellite Industry Report,” no. September, p. 33, 2014. [Online]. Retrieved from: http://www.sia.org/wp-content/uploads/2014/09/SSIR-September-2014-Update.pdf

[3] T.K. Priyambodo, A.E. Putra, M. Asvial, and R.E. Poetro, “IiNUSAT-1 : The 1 st Indonesian Inter-University Nano-Satellite for Research and Education,” In 2014 IEEE International Conference on Aerospace Electronics and Remote Sensing Technology, pp. 114–120, 2014.

[4] R. Votel and D. Sinclair, “Comparison of control moment gyros and reaction wheels for small Earth-orbiting satellites,” in Proceedings of the 26th Annual AIAA/USU Conference on Small Satellites, pp. 1–7, 2012.

[5] J. Chen, Z. Li, M.G. Gan, and G. Zhang, “Adaptive robust control for DC motors with input saturation,” IET Control Theory Appl., vol. 5, no. 16, pp. 1895–1905, Nov. 2011.

[6] J.L. Crassidis, Fundamentals of Spacecraft Attitude Determination and Control. New York Heidelberg,Heidelberg Dordrecht London: Springer, 2014.

[7] R. Fros, “How can I understand the saturation reaction wheel used in Attitude Control,” 2014.

[8] K. Kong, H.C. Kniep, and M. Tomizuka, “Output Saturation in Electric Motor Systems: Identification and Controller Design,” J. Dyn. Syst. Meas. Control, vol. 132, no. 5, pp. 051002-1-051002–8, 2010.

[9] X. Cao and B. Wu, “Indirect adaptive control for attitude tracking of spacecraft with unknown reaction wheel friction,” Aerospace science and technology, vol. 47, pp. 493–500, 2015.

[10] P. Guan, X. Liu, W. Zhang, and L. Xue, “The Direct Adaptive Fuzzy Robust Control for Satellite,” in Proceedings of 10th world Congress on Intelligent Control and Automation, pp. 36–41, 2012.

[11] S. Taniwaki and Y. Ohkami, “Experimental and Numerical Analysis of Reaction Wheel Disturbances,” JSME Int. J. Ser. C, vol. 46, no. 2, pp. 519–526, 2003.

[12] M.F. Mehrjardi, H. Sanusi, M. Alauddin, and M. Ali, “Developing a Proposed Satellite Reaction Wheel Model with Current Mode Control,” In 2015 International Conference on Space Science and Communication (IconSpace), pp. 0–3, 2015.

[13] Y. Yang, “Spacecraft Attitude and Reaction Wheel Desaturation Combined Control Method,” IEEE Transactions on Aerospace and Electronic Systems, vol. 53, no. 1, 2017.

[14] J. Li, M. Post, T. Wright, and R. Lee, “Design of Attitude Control Systems for CubeSat-Class Nanosatellite,” J. Control Sci. Eng., vol. 2013, no. April, pp. 1–15, 2013.

[15] Y.T. Xing, K.S. Low, S. Member, and M.D. Pham, “Distributed Model Predictive Control of Satellite Attitude Using Hybrid Reaction Wheels and Magnetic Actuators,” In 2012 IEEE Symposium on Industrial Electronics and Applications, pp. 230–235, 2012.

[16] A. Aydogan and O. Hasturk, “Adaptive LQR Stabilization Control of Reaction Wheel for Satellite Systems,” In 2016 14th International Conference on Control, Automation, Robotics and Vision (ICARCV), vol. 2016, no. November, pp. 13–15, 2016.

[17] J. Carlos, "Attitude Control Model for CubeSats," Iaa-Br-07-01, no. February, pp. 1–22, 2016.

[18] J. Li, M. Post, T. Wright, and R. Lee, "Design of Attitude Control Systems for CubeSat-Class Nanosatellite," J. Control Sci. Eng., vol. 2013, pp. 1–15, 2013.

[19] P. Suganthi, S. Nagapavithra, and S. Umamaheswari, "Modeling and Simulation of Close Loop Speed control for BLDC Motor," in Proc. IEEE Conference on Emerging Devices and Smart Systems (ICEDSS 2017), no. March, pp. 83–126, 2017.

[20] V. Carrara and H.K. Kuga, "Torque and Speed Control Loops Of A Reaction Wheel," 11th Int. Conf. Vib. Probl., no. September, pp. 9–12, 2013.

[21] F. Mitin and A. Krivushov, "Application of Optimal Control Algorithm for DC Motor," in 29th DAAM International Symposium on Intelligent Manufacturing and Automation, pp. 0762–0766, 2018.

[22] T.K. Priyambodo, A. Dharmawan, O.A. Dhewa, and N.A.S. Putro, "Optimizing control based on fine tune PID using ant colony logic for vertical moving control of UAV system," in AIP Conference Proceedings, vol. 1755, no. July, p. 170011, 2016.

[23] T.K. Priyambodo, A.E. Putra, and A. Dharmawan, "Optimizing control based on ant colony logic for Quadrotor stabilization," in 2015 IEEE International Conference on Aerospace Electronics and Remote Sensing Technology (ICARES), pp. 1–4, Dec. 2015.

[24] A. Dharmawan, A. Ashari, and A.E. Putra, "Quadrotor flight stability system with Routh stability and Lyapunov analysis," in AIP Conference Proceedings, vol. 1755, no. July, p. 170007, 2016.

[25] D. Hagen, Modelling and Controller Design considering Actuator Dynamics. Norway: Narvik University College, 2006.

[26] V. Izadi, M. Abedi, and H. Bolandi, "Verification of reaction wheel functional model in HIL test-bed," in 2016 4th International Conference on Control, Instrumentation, and Automation (ICCIA), no. January, pp. 155–160, Jan. 2016.